AAS 15-265

A NATURAL AUTONOMOUS FORCE ADDED IN THE RESTRICTED PROBLEM AND EXPLORED VIA STABILITY ANALYSIS AND DISCRETE VARIATIONAL MECHANICS

Natasha Bosanac,[*] Kathleen C. Howell,[†] and Ephraim Fischbach[‡]

With improved observational capabilities, an increasing number of binary systems have been discovered both within the solar system and beyond. In this investigation, stability analysis is employed to examine the structure of selected families of periodic orbits near a large mass ratio binary in two dynamical models: the circular restricted three-body problem and an expanded model that incorporates an additional autonomous force. Discrete variational mechanics is employed to determine the natural parameters corresponding to a given reference orbit, facilitating exploration of the effect of an additional three-body interaction and the conditions for reproducibility in the natural gravitational environment.

INTRODUCTION

With improved observational capabilities and techniques, an increasing number of binary systems have been discovered both within the solar system, in the form of asteroid pairs, and in extrasolar systems of planets and/or stars. In fact, approximately 16% of the asteroids that have been catalogued are members of binary or triple systems, none of which have yet been explored by a spacecraft.[1] Additionally, it is estimated that approximately 23% of detected exoplanets orbit within the vicinity of binary stars.[2] In each of these types of systems, many of the known binaries exhibit mass ratios larger than the Sun-planet and planet-moon combinations commonly examined within the solar system. Although the relative masses of the bodies in these binaries may be inferred via observational data or measurements, inaccuracies occur when each component is difficult to resolve individually. Since the dynamical environment in the vicinity of any binary system is inherently chaotic, such uncertainties may significantly affect the motion of a nearby small body.

In this investigation, periodic motions in the vicinity of a large mass ratio binary system are first explored within the context of the Circular Restricted Three-Body Problem (CR3BP). Although the dynamical environment near a binary star system may be modified by the presence of additional contributions such as gravitational radiation, the CR3BP offers a reasonable approximation for preliminary analysis of the motion of a nearby exoplanet. Meanwhile, for a binary asteroid, the restricted problem provides a simple, autonomous approximation to a higher-order gravitational field that may govern the motion of a spacecraft or a moonlet.[3] In each of these sample binary systems, the paths followed by comparatively small bodies are influenced by periodic orbits, which contribute to an underlying structure by attracting, bounding or repelling trajectories in their vicinity. The identification of stable orbits near a binary star system, for instance, may aid in modeling exoplanet motion that persists for a long time interval. Unstable orbits, however, could be used in a preliminary analysis of matter ejected from or captured by an asteroid pair. Stability analysis can be employed to identify suitable periodic orbits in each of these sample applications. Furthermore, the evolution of stability along a family of orbits also supports locating bifurcations, indicating structural changes or the formation of new families.

[*] Ph.D. Student, School of Aeronautics and Astronautics, Purdue University, 701 W. Stadium Ave., West Lafayette, IN 47907, USA.
[†] Hsu Lo Distinguished Professor of Aeronautics and Astronautics, School of Aeronautics and Astronautics, Purdue University, 701 W. Stadium Ave., West Lafayette, IN 47907, USA .
[‡] Professor of Physics, Department of Physics and Astronomy, Purdue University, 525 Northwestern Ave., West Lafayette, IN, 47907, USA.

An alternative dynamical model for the binary system is also derived based on the CR3BP, but extended to incorporate an additional autonomous term in the potential function, providing a Modified Circular Restricted Three-Body Problem (MCR3BP). Given the absence of experimental data gathered within the vicinity of a binary star, for example, it is possible that the gravitational field within this system might not be accurately modeled solely using pairwise gravitational forces. In this investigation, the presence of an additional three-body interaction is considered. Many-body forces are not an entirely new concept; in fact, the importance of three-body interactions in accurately modeling force fields on the atomic scale is well established in nuclear physics.[4] On a much larger scale, the motion of a small body orbiting a binary system serves as a new and interesting application for determining the characteristics of a three-body interaction in orbital dynamics. The additional three-body interaction, scaled using a constant k, is assumed to depend inversely on the product of the distances between the three bodies: the closer the bodies, the stronger the three-body interaction.[5] In this modified dynamical model, families of orbits still exist, but may evolve with the value of k in a manner that does not mimic the effect of the mass ratio of the binary, μ, thus providing potentially new solutions.

To visualize the stability across a given family of orbits, at various values of the natural parameters, a two-dimensional representation, similar to an exclusion plot, is employed. Exclusion plots are often used in physics to depict constraints on combinations of parameters.[6] This concept has been extended to represent the evolution of the stability of a family of periodic orbits near binary systems for various values of the natural parameters, μ and k.[7] From Floquet's theorem, reciprocal pairs of eigenvalues are frequently employed for qualitative classification of orbital stability. Through analysis of the stability index, i.e., the sum of each reciprocal pair of eigenvalues, three cases emerge: stability, positive instability and negative instability.[5] Each periodic orbit can, therefore, be represented on a composite stability plot as a point colored by the type of stability it exhibits. The resulting stability representation offers a simple visualization of the orbital stability of members across a given family, thereby enabling the detection of any structural changes, or bifurcations. Although these figures resemble Benest's stability diagrams, they differ primarily through their inclusion of the orbital period as a representative quantity.[7,8] This investigation presents exclusion plots for selected simply-periodic families at mass ratios in the range, $\mu = [10^{-6}, 0.50]$ for the CR3BP, which have been explored in depth in previous works by the authors.[7] In addition, composite stability representations are employed to visualize and summarize changes in the orbital stability across a given family when a three-body interaction is added to the dynamical environment of a binary system. These plots are constructed at a fixed value of the mass ratio, $\mu = 0.30$, for varying values of the scaling constant, k. Structural changes in selected families due to the presence of an additional autonomous force are then straightforwardly identified via a comparison between the corresponding stability plots.

Changes in the physical configuration of periodic orbits along a family, identified via composite stability representations, are then explored using discrete variational mechanics. In astrodynamics, this computational technique is typically used to determine optimal paths for a spacecraft under the influence of a control force.[9] In this investigation, however, the underlying formulation is applied to the search for values of the system parameters, μ and k, that correspond to the existence of a natural trajectory (i.e., no control forces) resembling a given reference path. The resulting constrained optimization problem delivers locally optimal solutions that supply approximations to trajectories in a wide variety of scenarios in both the CR3BP and MCR3BP, potentially avoiding some of the inherent sensitivities of a multiple shooting method when any natural parameters in a chaotic system are poorly known. Comparison between the geometries of the computed and reference orbits can then aid in identifying and exploring any potential effects of an additional autonomous force contribution. Although a three-body interaction is modeled in this investigation, a similar analysis can be performed for an alternative force that is both autonomous and derivable from a potential function, such as a time-averaged quantity or a higher-order gravitational term for a body fixed in a given coordinate frame.

DYNAMICAL MODELS

To facilitate exploration of the dynamical structure in the vicinity of a binary system, the CR3BP is employed. This dynamical model reflects the motion of a massless particle under the influence of the point-mass gravitational attractions of two primaries. In addition to the pairwise gravitational interaction typically employed to approximate the dynamics near a binary system, an autonomous term is added to the potential function of the CR3BP, producing the dynamical model in the MCR3BP. For this investigation, this additional autonomous potential contribution takes the form of a three-body interaction, as explored by Bosanac, Howell and Fischbach.[10] The MCR3BP is formulated similar to the traditional CR3BP, with the notation and general configuration consistent between the two models.[5] The form of the augmented potential in the MCR3BP influences the equations of motion, yielding a model that still admits an integral of the motion, and allows the existence of families of periodic orbits. Particular solutions, in the form of equilibrium points and zero velocity curves, are also available in this augmented model and still establish bounds on the motion.[5]

Circular Restricted Three-Body Problem

By convention, the body of interest, P_3, moves in the vicinity of the larger and smaller primaries, P_1 and P_2, with each body P_i possessing a mass m_i. In the CR3BP, a rotating coordinate frame, $\hat{x}\hat{y}\hat{z}$, is introduced and oriented relative to an inertial frame, $\hat{X}\hat{Y}\hat{Z}$. In the frame that rotates with the motion of the two primaries, the location of P_3, measured with respect to the barycenter, is written in terms of the nondimensional coordinates (x, y, z). Length quantities are nondimensionalized such that the distance between P_1 and P_2 is equal to a constant value of unity. In addition, time is nondimensionalized such that the mean motion of the primaries is equal to unity, while the characteristic mass quantity, m^*, is the sum of the masses of the primaries. The characteristic mass quantity yields nondimensional mass values for P_2 and P_1 equal to μ and $(1-\mu)$, respectively. In the rotating frame, the equations of motion for the spacecraft are written as:

$$\ddot{x} - 2\dot{y} = \frac{\partial U^*}{\partial x}, \qquad \ddot{y} + 2\dot{x} = \frac{\partial U^*}{\partial y}, \qquad \ddot{z} = \frac{\partial U^*}{\partial z} \tag{1}$$

where the pseudo-potential function, $U^* = \frac{1}{2}(x^2+y^2) + \frac{1-\mu}{r_1} + \frac{\mu}{r_2}$; then, $r_1 = \sqrt{(x+\mu)^2 + y^2 + z^2}$ and $r_2 = \sqrt{(x-1+\mu)^2 + y^2 + z^2}$. This autonomous pseudopotential function can be exploited to develop the energy integral that corresponds to the equations of motion as formulated in the rotating frame, and is equal to $C_J = 2U^* - \dot{x}^2 - \dot{y}^2 - \dot{z}^2$. This energy integral is the well-known Jacobi constant in the CR3BP.[11]

Modified Circular Restricted Three-Body Problem

Given a system configuration consistent with the CR3BP, derivation of the differential equations governing the motion of P_3 in the MCR3BP requires the definition of the potential function. In the rotating frame, the scalar potential corresponding to P_3, per unit mass, is assumed to consist of the following terms:

$$U_3 = \underbrace{\frac{1-\mu}{r_1} + \frac{\mu}{r_2}}_{\text{pairwise potential}} + \underbrace{\frac{k}{r_1 r_2}}_{\text{three-body potential}} \tag{2}$$

where k is the constant that scales the three-body potential term. Although the three-body interaction is assumed to depend inversely on the product of the distances between all three bodies, the distance between P_1 and P_2 is equal to a constant value of unity in this model. Accordingly, only r_1 and r_2 appear in the denominator of the three-body potential term. Since the magnitude and sign of the constant k are unconstrained, it is assumed that k can be selected as either positive, negative or zero. When the value of the constant k is equal to zero, the potential in the MCR3BP reduces to the CR3BP potential; if k is positive, the three-body interaction is attractive, while a negative value of the coefficient corresponds to a repulsive interaction.

From the definition of the potential function in Eq. (2), the equations of motion for P_3 are derived and a constant of motion is subsequently identified. The equations of motion in terms of the rotating frame are then written using the potential function as:

$$\ddot{x} - 2\dot{y} = \frac{\partial U_k^*}{\partial x}, \qquad \ddot{y} + 2\dot{x} = \frac{\partial U_k^*}{\partial y}, \qquad \ddot{z} = \frac{\partial U_k^*}{\partial z} \tag{3}$$

where the pseudopotential function is $U_k^* = \frac{1}{2}(x^2+y^2) + \frac{1-\mu}{r_1} + \frac{\mu}{r_2} + \frac{k}{r_1 r_2}$.[5] Since this pseudopotential is autonomous, a constant energy integral, C_k, exists and is equal to $C_k = 2U_k^* - \dot{x}^2 - \dot{y}^2 - \dot{z}^2$, reducing to the Jacobi constant in the CR3BP when $k = 0$.

Equilibrium Points

In the absence of an analytical solution to the nonlinear differential equations, significant insight into the dynamical environment emerges from particular solutions. In the rotating frame of the CR3BP, there exist five equilibrium points, labelled L_i, for $i = 1, 2, 3, 4, 5$ and their relative locations are identified by green dots in Figure 1(a) for a system with a mass ratio of $\mu = 0.30$. At this mass ratio, for $k = [-0.20, 0.70]$, the five planar L_i still exist and are perturbed from their locations in the CR3BP, except for L_4 and L_5 which no longer exist within the plane of motion of the primaries for $k < -0.1985$. For positive values of k, the planar equilibrium points are numerically computed and located in the MCR3BP in Figure 1(a) using blue dots, while red dots are used to depict each L_i for negative values of k. Purple dots correspond to two additional equilibrium points that exist over the small range of values $k \approx [-0.1985, -0.1839]$.[12] Analysis of Figure 1(a) reveals that, for an increasingly attractive three-body interaction, i.e., larger positive values of k, the collinear equilibrium points are located farther from P_2.[10] In addition, the triangular equilibrium points, L_4 and L_5, are no longer located at the vertices of equilateral triangles as in the CR3BP. For negative values of k, however, the equilibrium points each exist closer to P_2. To understand the appearance and disappearance of an additional pair of equilibrium points, labelled L_{4b} and L_{5b}, over a small range of negative values of k, a summary of the stability of each equilibrium point is useful. In Figure 1(b), the two colored bars for each of the labelled L_i reflect a qualitative measure of the linear stability of each of the two planar modes. Specifically, blue portions along a bar indicate oscillatory modes, while red reflects the presence of a stable and unstable pair of eigenvalues at the corresponding values of k. Across the range $k = [-0.20, 0.70]$, indicated along the horizontal axis, this figure reveals that the stability of L_2 and L_3 remains qualitatively unchanged. For L_1, however, the oscillatory mode, which contributes to the existence of the planar Lyapunov family in the CR3BP, undergoes a pitchfork bifurcation at $k \approx -0.1839$. In addition to a change in the stability of L_1 due to this bifurcation, L_{4b} and L_{5b} are created and each possess one pair of imaginary eigenvalues. As k becomes increasingly negative, the locations of L_{4b} and L_{5b}, indicated by purple dots in Figure 1(a), symmetrically evolve away from L_1 on the x-axis, approaching L_4 and L_5 until the critical value of $k \approx -0.1985$, when the pairs of equilibrium points meet. While these equilibrium points represent constant solutions to the equations of motion, additional types of steady-state solutions also exist: periodic orbits, quasi-periodic orbits, and chaotic motion.[13] Each of these motions can be examined using concepts developed in dynamical systems theory.[10]

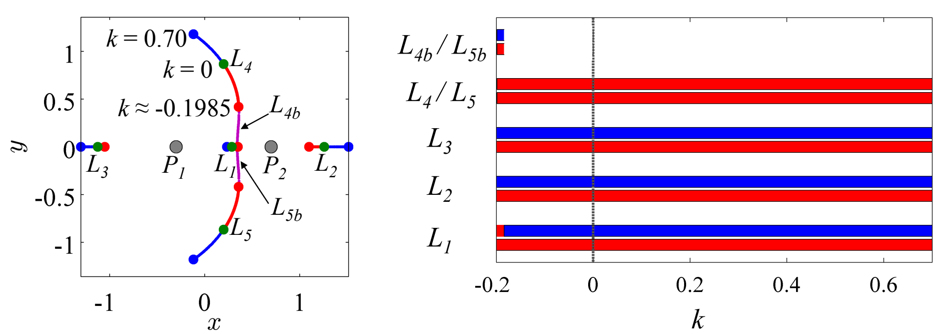

(a) Location of planar equilibrium points in the CR3BP (green) and the MCR3BP for: $k > 0$ (blue dots), $k < 0$ (red dots), and $-0.1985 < k < -0.1839$ (purple).

(b) Stability of two planar modes for each equilibrium point as a function of k, with blue indicating oscillatory modes and red corresponding to a pair of stable and unstable eigenvalues.

Figure 1: Equilibrium points in the MCR3BP.

PERIODIC ORBITS

Of particular interest in this investigation are planar, periodic solutions, which lie within the plane of motion of the two primaries and repeat after a period, T. In fact, the dense set of periodic orbits in both the CR3BP and the MCR3BP, exist in continuous families and form the underlying structure of the phase space:

a stable orbit attracts or bounds trajectories in its vicinity, while trajectories near an unstable orbit flow away from the orbit.[14] In the vicinity of stable periodic orbits are quasi-periodic orbits, which trace out the surface of a torus. This boundedness may be approximately retained in a higher-fidelity gravitational environment. Unstable orbits, however, may also supply transfer mechanisms between various regions of the phase space. Thus, identifying periodic orbits and evaluating their stability delivers significant insight into the underlying structures in their vicinity. Periodic orbits can encircle either one or both primaries in any direction in the rotating frame. For clarity, some definitions are useful. At any instant, a trajectory as viewed in the rotating frame with an angular momentum vector with respect to one of the primaries in the $+\hat{z}$ direction is defined as prograde.[5] Correspondingly, a state along a retrograde path possesses an angular momentum vector directed in the $-\hat{z}$ direction. In the rotating frame, a periodic orbit can appear to wind about one of the primaries in an entirely prograde or retrograde direction, or alternate between the two directions as it encircles the primaries.

Stability

The stability of a periodic orbit is typically deduced from the monodromy matrix, defined as the state transition matrix propagated for precisely one period of the orbit.[15] Given a reference planar periodic orbit, the solution that approximates a nearby arc is determined using the linear variational equations of motion. The solution describing the relative neighboring arc is written as $\delta\bar{x}(t) = \mathbf{\Phi}(t,0)\delta\bar{x}(0)$ where $\delta\bar{x}(0)$ is the vector variation with respect to the initial state along the reference path and $\mathbf{\Phi}(t,0)$ is the state transition matrix, essentially a linear mapping from $t_0 = 0$ to a time t.[16] Via Floquet theory, each planar periodic orbit, which exists in the full three-dimensional space, possesses a monodromy matrix, $\mathbf{\Phi}(T,0)$, that can be decomposed into six eigenvalues, λ_i, and their associated eigenvectors.[16] Two of the eigenvalues are equal to unity due to periodicity. The other four nontrivial eigenvalues, which exist in reciprocal pairs due to the symplectic and time-invariant properties of the state transition matrix, may be represented in the form $\lambda = a \pm bi$, in terms of two real numbers, a and b. For a planar orbit, one nontrivial pair of eigenvalues corresponds to an in-plane mode, while the other corresponds to out-of-plane stability. A stability index, s, can also be defined as the sum of each pair of reciprocal eigenvalues.[5] Depending on the value of a and b, three specific types of eigenvalues emerge: real, complex, and imaginary. From the Lyapunov definition of stability, a periodic orbit that exhibits stability possesses a pair of complex or imaginary eigenvalues, $\lambda_1, \lambda_2 = a \pm bi$, and, therefore, a real-valued stability index between $s = -2$ and $s = +2$. A pair of reciprocal eigenvalues, $|\lambda_1| = a > 1$ and $|\lambda_2| = 1/a < 1$, however, correspond to instability.[15] Unstable periodic orbits can, therefore, be identified by at least one stability index with a magnitude greater than two. Since the stability of a planar periodic orbit reflects the behavior of solutions within its vicinity, the parameter s reduces the complexity in visualizing the stability of orbits along a family at various values of the mass ratio.

Bifurcations

In the CR3BP, periodic orbits exist in families that, for a given mass ratio, depend upon the energy constant, C_k. Varying C_k, the natural parameter, directly modifies the vector field and, therefore, its infinite set of solutions. In dynamical systems, a bifurcation may occur as a natural parameter is varied and can result in either a change in the stability of the periodic orbits along a family, the formation of a new family of periodic orbits, or termination of the current family.[17] Since the stability of a periodic orbit reflects the behavior of nearby trajectories, local bifurcations are detected through the pairs of nontrivial eigenvalues of the monodromy matrix corresponding to each periodic orbit along a family, reflected by the parameter s as it passes through any critical values.

Although many possible bifurcations exist, two types emerge within the dynamical environment that is the focus of this investigation: tangent and period-multiplying bifurcations. A family of periodic orbits undergoes a tangent bifurcation when the qualitative stability characteristics of its orbits change as its eigenvalues pass through the critical values $\lambda_1 = \lambda_2 = +1$. Simultaneously, the stability index passes through $s = +2$. Depending on the type of tangent bifurcation, the resulting change in stability may be accompanied by the creation of families of orbits with a similar period or by the intersection with another family of orbits. During a period-multiplying bifurcation of multiplicative factor m, a family of period-mq orbits emerges from a family of period-q orbits. Here, q is the integer corresponding to the number of times a periodic orbit encircles a reference location. Employing properties of the state transition matrix, this bifurcation is detected when a pair of eigenvalues from the period-q orbits along a family pass through the first and $(m-1)$-th complex roots of unity, and when the stability index passes through the critical value, $s = 2\cos\left(\frac{2\pi}{m}\right)$. The special case of a period-doubling bifurcation occurs when the stability index passes through $s = -2$. This bifurcation can be accompanied by a change in stability if the corresponding pair of eigenvalues split off onto the real axis.

COMPOSITE STABILITY REPRESENTATION

To visualize the evolution of the orbital stability across a family, a simple composite representation is constructed. The in-plane and out-of-plane stability indices across a family of orbits at a given mass ratio and a value of the scaling constant, k, each form a single curve when plotted against the orbital period. Often, the stability index along these curves exhibits a number of turning points and a large range of values. Accordingly, simply overlaying these complex curves at various values of a natural parameter can hinder any exploration of the stability characteristics along the family. A simplified representation of the stability in a two-parameter space, such as (μ, T) or (k, T), however, enables clearer visualization, and aids in the examination of the evolution of the family. Although only a short summary is presented in this paper, these composite stability representations are discussed in detail and explored within the context of the CR3BP by Bosanac, Howell and Fischbach for a variety of orbit families.[7]

The composite stability representation employed in this investigation is constructed by simply assessing a qualitative measure of the stability along a family. Since the eigenvalues of the monodromy matrix reflect a linear approximation of the dynamics, they can only be used to qualitatively determine the type of stability exhibited by a periodic orbit in the nonlinear dynamical environment in either the CR3BP or MCR3BP. In particular, each orbit along a family is classified using either the in-plane or the out-of-plane stability index, s: stable, for $s = [-2, 2]$; positive unstable, for $s > 2$; and negative unstable, for $s < -2$. The point representing a single periodic orbit in the two-parameter space, (μ, T) or (k, T), can, therefore, be colored by the type of stability it exhibits. In this investigation, a stable orbit is assigned the color blue, a positive unstable orbit is colored red and negative instability is represented by the color purple. Since multiple periodic orbits may possess the same orbital period, points corresponding to stable periodic orbits are brought to the front of each plot, as they correspond to the motion of interest in this investigation. Thus, for a given value of μ, a complex curve encompassing a large range of values of s is reduced to a single line that is overlaid for various mass ratios within a specified range, forming a useful, two-dimensional composite stability representation.

To demonstrate the construction of a composite stability representation, consider a simply-periodic retrograde family of orbits in the CR3BP that exists within the exterior region, far from both primaries. The corresponding stability representation for a portion of this family possessing periods below 20 nondimensional time units, is depicted in Figures 2(a) and 2(b) for the in-plane and out-of-plane stability, respectively. To facilitate visualization of the evolution of a family across a large range of mass ratios, a mixed linear-log scale is employed to represent μ on the vertical axis. Specifically, mass ratios in the range $\mu = [0.10, 0.50]$ are plotted via a linear scale, while mass ratios in the range $\mu = [10^{-6}, 0.10)$ are displayed using a log scale. The boundary between these two scales is indicated by a black dashed line. For comparison, selected systems with known mass ratios are also indicated on the plots that represent the three-dimensional stability index, such as in Figure 2(b). In addition, sample periodic orbits are displayed in the margins at selected values of the natural parameters and period to reflect the configuration of family members in physical space as viewed in the rotating frame. Recall that stable orbits are located within the blue regions of these composite representations, while negative instability is indicated by purple structures and positive unstable orbits are located within the red regions. Colored structures, therefore, reflect the stability of periodic orbits along a family, as well as the occurrence of some bifurcations. If the family is closed or reduces to an equilibrium point, for example, these "dynamical barriers" are represented via gray shading, which indicates that the family cannot extend into the shaded region of the (μ, T) or (k, T) space. To limit the computational time and effort, members of each family are only computed until they pass through a predefined maximum period, pass within some radius of either primary, or become difficult to compute numerically. Since the CR3BP and MCR3BP are inherently nonlinear, it may not be possible to accurately predict the stability across any portions of the family that are not computed. Accordingly, any white regions of space, at a given value of μ or k, indicate

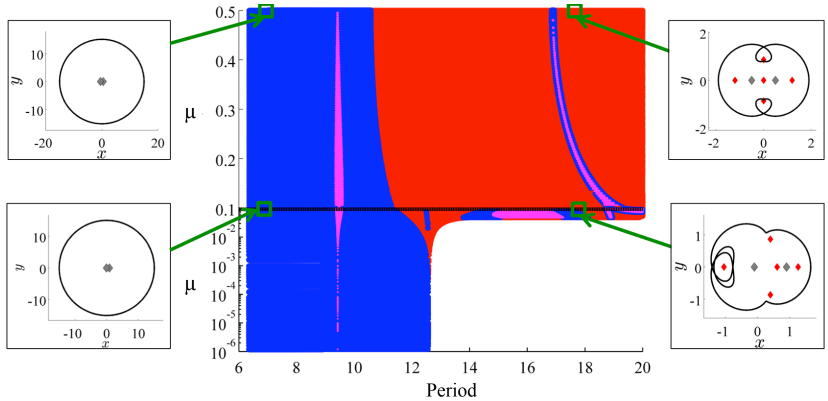

(a) In-plane stability.

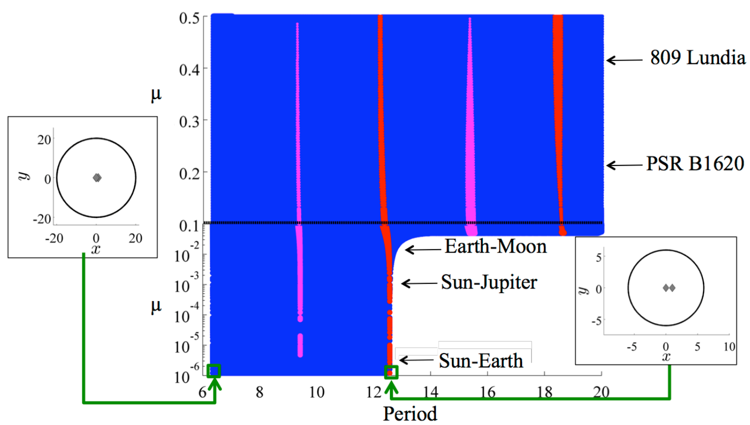

(b) Out-of-plane stability.

Figure 2: Stability representation for retrograde orbits in the exterior region for $\mu = [10^{-6}, 0.5]$ and $k = 0$. Orbital stability is indicated via color: stable (blue), positive unstable (red), and negative unstable (purple).

that the family may not be computed in its entirety. Due to the possible existence of turning points along a family, periodic orbits that are not computed may possess periods either within or beyond the colored regions. For computed portions of a family, however, a composite stability representation allows for straightforward visualization of the stability across a family for varying values of a natural parameter, such as μ or k.

CONSTRAINED OPTIMIZATION USING DISCRETE VARIATIONAL MECHANICS

To supplement the use of composite stability representations in observing changes in the periodic orbits along a family, discrete variational mechanics is employed to explore the effect of an additional force contribution that is both autonomous in the rotating frame of the CR3BP and may be derived from a potential function. In this investigation, it is of interest to determine if the effect of varying k, the scaling constant corresponding to a three-body interaction with an assumed form, is reproducible in the CR3BP by varying the mass ratio, μ. Such analysis may reveal if the effect of an additional term is unique, enabling identification of periodic solutions that may not exist in the CR3BP. To explore the effect of an autonomous force term, discrete variational mechanics is leveraged to determine a combination of natural parameters, (μ, k), that supplies a trajectory which closely resembles a given reference path. As opposed to collocation or a multiple-shooting method, which require the continuous dynamics of a system be exactly satisfied at a discrete set of nodes or along multiple trajectory arcs, the discrete variational methodology begins with a discretization of the action integral.[18] A discrete version of Hamilton's principle, which involves the variation only at a finite set of nodes along a discretized path, is then used to constrain the motion within a dynamical system.[9] This method does not require integration, and may alleviate the effect of numerical sensitivities induced by a poor initial guess. To establish a framework for this methodology, some background is offered, followed by a discussion of the application of discrete variational mechanics to the construction of natural trajectories in both the CR3BP and the MCR3BP.

Variational Principles for Continuous Time Systems

Prior to a discussion of discrete variational concepts, fundamental variational principles in Lagrangian mechanics are summarized within the context of continuous time systems. First, consider a mechanical system which can be described by a Lagrangian, $L(q(t), \dot{q}(t))$, for the generalized coordinates q and generalized velocities $\dot{q}$. Integrating this continuous Lagrangian along a path followed by the system from a time $t_0 = 0$ to a subsequent time t yields the following functional, typically identified as the action integral:[19]

$$A = \int_{t_0}^{t} L(q(t), \dot{q}(t))dt \tag{4}$$

By Hamilton's principle, any actual path $q(t)$ that could be followed in a holonomic system results in a stationary action integral with respect to path variations, for fixed endpoints.[20] Mathematically, this statement is expressed as:

$$\delta A = \delta \int_{t_0}^{t} L(q(t), \dot{q}(t))dt = \int_{t_0}^{t} \left(\frac{\partial L}{\partial q} - \frac{d}{dt}\left(\frac{\partial L}{\partial \dot{q}}\right)\right) \delta q dt = 0 \tag{5}$$

For this statement to be true for all nonzero variations along the path $q(t)$, the integrand of Eq. (5) must equal zero, thereby recovering the continuous time Euler-Lagrange equations:

$$\frac{\partial L}{\partial q} - \frac{d}{dt}\left(\frac{\partial L}{\partial \dot{q}}\right) = 0 \tag{6}$$

Thus, any natural trajectory followed by a continuous time system must satisfy the Euler-Lagrange equations, a well-known concept in Lagrangian mechanics.[19]

Discrete Variational Mechanics

In the absence of an analytical solution for the motion of a system, only a discretely sampled path is available, requiring modification of the continuous variational concepts in Lagrangian mechanics to accommodate discrete time as investigated by Marsden and West.[21] Sampling of a natural trajectory inherently occurs during numerical integration, or even observation. Consider, for this investigation, discrete sampling occurring N times at constant intervals, of length h, for a total time $t = (N-1)h$. Then, a continuous path $q(t)$ is approximated by a discrete path $\tilde{q}$ described by the set of generalized coordinates $q_i = \tilde{q}(ih)$ where $i = 0, 1, ..., N-1$.[21] Velocities along the path are replaced by finite difference approximations, such as $\dot{q}_i \approx \frac{(q_{i+1} - q_i)}{h}$, which converge to the true velocity along a nonlinear path as h approaches zero. Analogous to the theory associated with continuous time systems, a discrete time Lagrangian can then be defined as $L_d(q_i, q_{i+1}, h)$, approximating the integral of the true Lagrangian, $L(q(t), \dot{q}(t))$, over the i-th time interval of length h as the system travels from q_i to q_{i+1}.[9] Since $L_d(q_i, q_{i+1}, h)$ is calculated as a numerical integral, an appropriate quadrature rule must be selected to approximate the continuous dynamics of the system.[21] Once an expression for $L_d(q_i, q_{i+1}, h)$ is defined, a discrete action can then be constructed using the summation of the discrete Lagrangian over all $N-1$ time intervals, such that:

$$A_d = \sum_{i=0}^{N-2} L_d(q_i, q_{i+1}, h) \approx \int_{t_0}^{t} L(q(t), \dot{q}(t))dt \tag{7}$$

Applying Hamilton's principle to this expression for the discrete action, and using summation by parts, a discrete time counterpart to Eq. (5) is available:

$$\delta A_d = \delta \sum_{i=0}^{N-2} L_d(q_i, q_{i+1}, h) = \sum_{i=1}^{N-2} \left[\left(\frac{\partial L_d(q_i, q_{i+1}, h)}{\partial q_i} + \frac{\partial L_d(q_{i-1}, q_i, h)}{\partial q_i} \right) \delta q_i \right] = 0 \tag{8}$$

From this expression, for the discrete action to be stationary with respect to all path variations, with fixed endpoints, the discrete Euler-Lagrange equations must be satisfied across each time interval $[t_i, t_{i+1}]$:

$$\frac{\partial L_d(q_i, q_{i+1}, h)}{\partial q_i} + \frac{\partial L_d(q_{i-1}, q_i, h)}{\partial q_i} = 0 \tag{9}$$

for $i = [1, N-2]$. Note that this form of the discrete Euler-Lagrange equations is only true for systems with no external forcing, as is the case for the dynamical model employed in this investigation. Straightforward modifications to incorporate forcing terms into these discrete equations, however, have been presented and used by numerous authors in previous works.[9]

Formulation of Constrained Optimization Problem

The concepts from discrete variational mechanics provide a set of constraints, in the form of the discrete Euler-Lagrange equations, that can be used in a constrained optimization problem to determine a discrete path minimizing a given objective function. In a continuous time system, this objective function takes the form of an integral over the path $q(t)$ from time t_0 to t, given by $J(q, \dot{q}) = \int_{t_0}^{t} C(q(t), \dot{q}(t))dt$, for some specified function C. However, this infinite dimensional functional $J(q, \dot{q})$ can be transformed into a finite dimensional objective function by replacing the integral with a summation of discrete cost functions, each evaluated at the N nodes along the discrete path:

$$J_d(\tilde{q}) = \sum_{i=0}^{N-2} C_d(q_i, q_{i+1}, h) \approx \int_{t_0}^{t} C(q(t), \dot{q}(t))dt \tag{10}$$

Since this approximation implies that the discrete cost function at the i-th node is a numerical integral of the continuous function C over the i-th time interval, an appropriate quadrature rule can be selected to produce an expression for $C_d(q_i, q_{i+1}, h)$.[9] Of course, the order of the selected quadrature rule influences the rate of convergence of the error between $J_d(\tilde{q})$ and $J(q, \dot{q})$ as the time interval is reduced.

Any discrete path that optimizes this objective function must also satisfy the discrete Euler-Lagrange equations, which reflect the dynamics of the system. A finite dimensional constrained optimization problem is, therefore, summarized as:

$$\min \qquad J_d(\tilde{q}) = \sum_{i=0}^{N-2} C_d(q_i, q_{i+1}, h)$$

subject to the constraints from Eq. (9), reflecting the system dynamics:

$$\frac{\partial L_d(q_i, q_{i+1}, \mu, k, h)}{\partial q_i} + \frac{\partial L_d(q_{i-1}, q_i, \mu, k, h)}{\partial q_i} = 0 \qquad\qquad i = 1, ..., N-2$$

At each of the interior nodes, the resulting constrained optimization problem can affect the two position variables in this planar problem, $q_i = (x_i, y_i)$. Furthermore, h, μ, and k are all treated as variables to allow modification of both the orbital period and the dynamical environment, resulting in a total of $2N + 3$ design variables. Additional position and/or momentum boundary conditions can also be applied.[9] To enforce both symmetry and periodicity along an approximate path, an extra node is added to the discrete path and position boundary conditions are employed. Next, equality constraints can be applied to h, μ, or k depending upon the application. The resulting constrained optimization problem, formulated using discrete variational mechanics, is straightforward to apply to the computation of a natural trajectory in the MCR3BP, assuming a constant time interval between each node and a constant value of each of the natural parameters, μ and k.

To construct the constraint relationships that enforce natural motion in either the CR3BP or MCR3BP, a discrete Lagrangian, approximating the integral of the exact Lagrangian over each of the $N - 1$ segments between two nodes, must first be defined. In this investigation, the numerical integral supplying the discrete Lagrangian is approximated using the midpoint rule:

$$L_d(q_i, q_{i+1}, h) = hL\left(\frac{q_i + q_{i+1}}{2}, \frac{q_{i+1} - q_i}{h}\right) \tag{11}$$

where L_d is constructed using the average of the position variables evaluated at both the left and right boundaries of the i-th segment, with a velocity that is calculated using a first-order finite differencing. For the MCR3BP, the continuous Lagrangian of the system is straightforwardly written as:

$$L(x, y, \dot{x}, \dot{y}) = \frac{1}{2}(\dot{x} - y)^2 + \frac{1}{2}(\dot{y} + x)^2 + \frac{1-\mu}{r_1} + \frac{\mu}{r_2} + \frac{k}{r_1 r_2} \tag{12}$$

reducing to the Lagrangian of the CR3BP for $k = 0$. Once this continuous Lagrangian is employed to evaluate the discrete Lagrangian across each segment using the midpoint rule in Eq. (11), the resulting expressions for L_d over the i-th and (i-1)-th segments are differentiated and combined using Eq. (9) to form the discrete Euler-Lagrange equations, which must be satisfied for all discrete path variations, given fixed endpoints.

The objective function to be minimized must also be defined. In the examples in this investigation, the desired solution should resemble a given reference path. To formulate a useful cost function, note that the motion along a periodic orbit can be influenced by the stability and existence of equilibrium points, sometimes even forming loops in their vicinity. As the value of k or μ is varied, these equilibrium points may appear at different locations in the configuration space. Accordingly, a converged solution may resemble a reference path in its general behavior and appearance, even if it does not possess exactly the same path in the (x, y) configuration space. A continuous cost function for a point located at $q = (x, y)$ is, therefore, defined using the distance from a corresponding point along the reference path, $q_{ref} = (x_{ref}, y_{ref})$, such that $C(x, y) = (x - x_{ref})^2 + (y - y_{ref})^2$. A discrete cost function, $C_d(q_i, q_{i+1}, h)$, is then determined by applying the midpoint rule to this continuous cost function. The resulting objective function, constructed by summing $C_d(q_i, q_{i+1}, h)$ across all segments, is used in the sequential quadratic programming algorithm available in MATLAB's *fmincon* routine to produce a converged solution that is located close to the reference path in a dynamical environment described by the natural parameters, (μ, k).

APPLICATION OF STABILITY ANALYSIS AND DISCRETE VARIATIONAL MECHANICS: EXPLORING THE EFFECT OF AN ADDITIONAL AUTONOMOUS FORCE CONTRIBUTION

By combining composite stability representations with the capability to reproduce a desired trajectory at specified values of the natural parameters, μ and k, via discrete variational mechanics, it is possible to explore the effect of an additional three-body interaction force. First, composite representations of the in-plane and out-of-plane stability indices are employed to examine the evolution of selected families in each of the following cases: varying μ within the range $\mu = [10^{-6}, 0.50]$, while k is held fixed at a value of zero; and allowing the strength of the three-body interaction to vary within the range $k = [-0.20, 0.70]$, for $\mu = 0.30$. Since the orbital stability within and out of the plane can be decoupled for planar periodic orbits, the two corresponding stability indices are isolated and examined separately in each case. Using each composite stability representation, qualitative changes across each family are identified using colored structures that can reveal changes in the stability. Orbits of interest that are identified using these exclusion plots are isolated and input to the constrained optimization problem. This process is used to explore selected orbits and assess their existence in the MCR3BP as unique, or their potential to be approximately reproduced in the CR3BP by perturbing the mass ratio. The examples considered in this investigation involve two simply-periodic families: large retrograde orbits in the exterior region, and prograde orbits about the largest primary.

Retrograde Circumbinary Orbits

If observational data suggests that a moonlet, for example, follows a circumbinary orbit in a binary asteroid system, encircling both primaries, a simply-periodic family of retrograde orbits that exist in the exterior region in the CR3BP may be of interest. The composite representations in Figures 2(a) and 2(b) are used to assess the effect of changes in the mass ratio on the evolution of this family. First, consider the in-plane stability along this family of orbits. Note that these simply-periodic retrograde orbits do not collapse to a singularity. Instead, this family originates at its minimum energy value within the homoclinic tangles of the manifolds of the L_2 Lyapunov orbits.[7] Below periods of approximately $T = 11.3$ nondimensional time units, the majority of members of this family are stable within the plane of motion of the primaries, as indicated by the large blue regions in Figure 2(a). There does, however, exist a thin purple band of negative instability centered about $T = 9.42$, where the stability curve plunges below $s = -2$, creating two planar, period-doubling bifurcations that persist over the range of mass ratios considered in this investigation. The blue region to the right of this purple structure is bound on its other side by a red region. Accordingly, the retrograde exterior family undergoes a variety of planar period-multiplying bifurcations as the stability index encompasses the range of values $s = [-2, 2]$ within this blue region. As the orbital period is increased, this evolution of the stability index corresponds to a pair of complex conjugate eigenvalues moving from -1 to +1, along the unit circle. Beyond a period of approximately 11.3 time units, the simply-periodic retrograde exterior family is predominantly unstable in the plane of motion of the primaries, for large values of μ. There is, however, a thin blue and purple structure that indicates the presence of stable members over a small range of high orbital periods, as the stability curve plunges below $s = -2$. Since this stable region is curved, and does not form a vertical band, the values of the orbital period corresponding to these stable members is considered sensitive to changes in large values of the mass ratio. As an example of the utility of such analysis, if the mass ratio of a binary is inaccurately known, it may be difficult to determine if, for a fixed orbital period between 16.84 and 19.37 nondimensional time units, simply-periodic retrograde motions resembling orbits in this family - that exhibit in-plane stability - could be followed by a small body for a long time interval.

For large mass ratios in the range $\mu = [0.10, 0.50]$, the three-dimensional stability associated with the simply-periodic retrograde family of orbits in the exterior region exhibits alternating structures that appear at almost regular intervals along the orbital period. By examination of Figure 2(b), members of this family are predominantly stable in a direction that is perpendicular to the plane of motion of the primaries. There are, however, thin regions of negative and positive instability that are embedded within this figure. The alternating configuration of these structures, which appear to nearly repeat approximately every 2π time units in the orbital period, indicates that the out-of-plane stability index is oscillatory with respect to the orbital period. This oscillation in the three-dimensional stability across the family appears correlated to the presence of loops that form along the orbits in this retrograde exterior family near L_4 and L_5: as the orbital period is increased by 2π time units, the orbits in this family form additional nested loops near the triangular equilibrium points in a fractal manner. In fact, each new set of loops that forms near L_4 and L_5 corresponds to the orbit completing an additional revolution around the system barycenter when viewed in an inertial frame. This observation appears consistent for values of μ where the period of orbits in this family grows large.

Using the evolution of the retrograde exterior family in the CR3BP as a reference, the effect of a three-body interaction can be explored using the same type of stability analysis by varying the value of k, while holding the mass ratio fixed at $\mu = 0.30$. Figures 3(a) and 3(b) depict the composite stability representation for values of k within the range $k = [-0.20, 0.70]$. Since the two stability indices can be decoupled for planar periodic orbits, initially consider the in-plane stability along the family. As k is increased in the positive direction, and the three-body interaction is increasingly attractive, the negative unstable periodic orbits that exist in the purple structure near $T = 9.42$ encompass a wider range of orbital periods. In comparison to the CR3BP, this effect occurs for a decreasing mass ratio close to $\mu = 0.30$. A similar expansion in the range of periods corresponding to negatively unstable orbits also occurs for decreasing values of k. Thus, the variation in the range of orbital periods corresponding to each region of stable or unstable orbits due to a nonzero k does not appear to exactly mimic the effect of modifying the mass ratio value around $\mu = 0.30$. Despite the varying size of these blue and purple structures, their consistent presence for orbital periods below approximately 10 nondimensional time units suggests that the three-body interaction may not qualitatively impact the in-plane stability curve of this family at low orbital periods. Similarly, the thin blue and purple structures that occur at higher orbital periods, inherited from the CR3BP at $k = 0$, seem to persist for the majority of k values represented in the composite stability representation. At large negative values, however, the thin blue structure at periods close to 25 nondimensional time units, seems to undergo a significant change in the corresponding orbital periods for a small perturbation in the value of k. In fact, this structural change is also apparent in the out-of-plane stability representation in Figure 3(b) as it impacts both the thickness and location of the purple and red structures. This significant change in the stability indices suggests that the physical characteristics of the orbits themselves may be influenced by the presence of a three-body interaction force.

Observing the physical configuration of the retrograde exterior orbits in the margins of the composite stability representations for the MCR3BP reveals some change in the appearance of the orbits as k varies. In

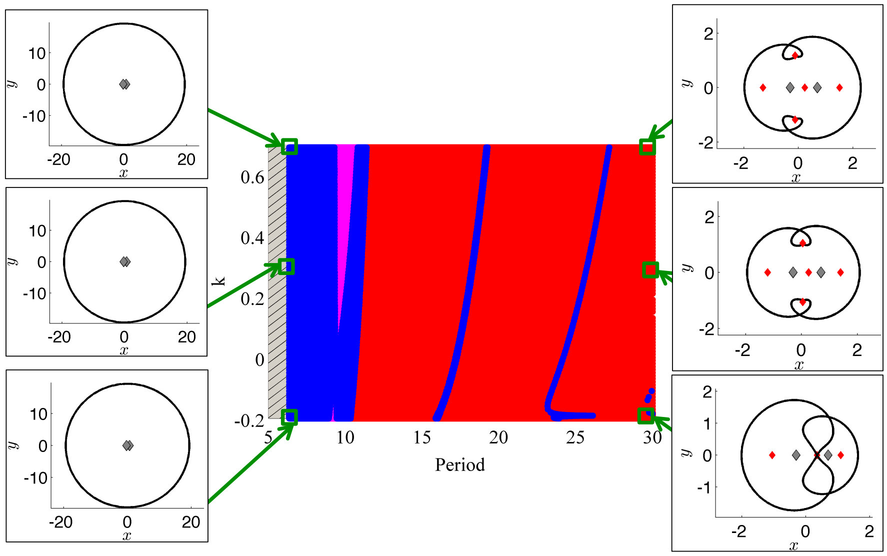

(a) In-plane stability.

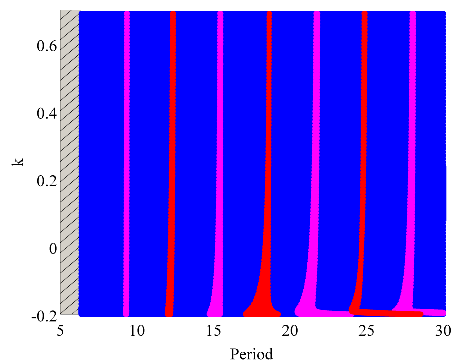

(b) Out-of-plane stability.

Figure 3: Stability representation for the selected family of retrograde orbits in the exterior region for $k = [-0.20, 0.70]$ and fixed mass ratio, $\mu = 0.30$. Orbital stability is indicated via color: stable (blue), positive unstable (red), and negative unstable (purple).

Figure 3(a), low period orbits plotted to the left of the composite stability representation appear similar in their near-circular shape and large size, presumably because they exist far from the two primaries. However, the difference in the evolution of the retrograde exterior family between the CR3BP and MCR3BP is apparent through examination of orbits with a larger period. In the CR3BP, Figure 2(a) reveals that, as the orbital period increases along the family for large values of the mass ratio, the orbits evolve towards the primaries and form loops in the vicinity of L_4 and L_5. Increasing the orbital period even further, in multiples of 2π, additional loops form near these two equilibrium points in a fractal manner. In the MCR3BP, however, both L_4 and L_5 no longer exist at the vertices of equilateral triangles with respect to the two primaries. Accordingly, the loops that form along these retrograde orbits appear shifted in configuration space, as evident in the margins of 3(a). This effect of the three-body interaction can be attributed to the varied locations of the equilibrium points themselves. Furthermore, for large negative values of k close to $k = -0.20$, these loops tend to exhibit 'pointed tips' which evolve towards L_1, as evident in the zoomed-in view in Figure 4. To understand this significant change in the physical configuration of the retrograde exterior family, recall that a straightforward stability analysis for the collinear equilibrium points assuming large negative values of k reveals a change in the stability of L_1. In fact, at the critical value of $k \approx -0.1839$, the pair of eigenvalues corresponding to the planar oscillatory mode inherited from the CR3BP undergoes a stability change, resulting in L_1 possessing only stable and unstable modes, and causing the disappearance of the L_1 Lyapunov family. These changes to the equilibrium points and, therefore, their manifolds and the underlying dynamical structure of the MCR3BP, influence the physical configuration of this family of orbits. In fact, this observation suggests that the effect of the three-body interaction on these retrograde exterior orbits at large negative values of k may not be exactly reproduced within the CR3BP, but, rather, mimicked. Accordingly, discrete variational mechanics is used to explore the effect of this additional force and if it is approximately reproducible in the CR3BP.

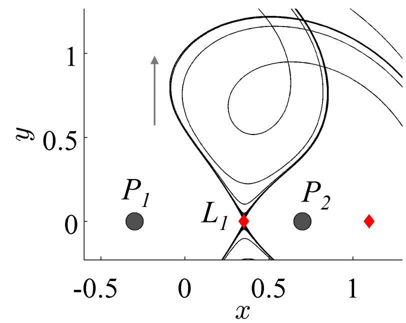

Figure 4: Loops forming along the retrograde exterior family for a large repulsive three-body interaction, with pointed tips directed towards L_1 for $\mu = 0.30$ and $k = -0.20$.

To test the validity of using discrete variational mechanics to predict the existence of periodic orbits in the MCR3BP, a known orbit with 'pointed tips' is recovered, along with the corresponding values of the natural parameters μ and k. First, an orbit of period $T = 26.26$ nondimensional time units is selected from the bottom right of the composite stability representation in Figure 3(a). This orbit is known to exist in the MCR3BP with a mass ratio $\mu = 0.30$ and $k = -0.20$. As depicted in Figure 5(a), this orbit is discretized into 500 nodes using a constant time step, with each node represented as a black dot. In this figure, the primaries are located using gray filled circles, while the equilibrium points in the MCR3BP are identified via red filled diamonds. The plotted discrete reference path is supplied as an initial guess for the constrained optimization problem, along with the natural parameters $\mu = 0.32$ and $k = 0.01$, which represent a poor guess for μ and k. While the value of the mass ratio is constrained to possess a value of $\mu = 0.30$, both the time step h and value of k are allowed to vary. The converged solution, overlaid on the reference path in Figure 5(b) using blue circles, returns a discrete path that appears to closely match the original reference path, to within a small numerical error. In addition, the locally optimal solution that minimizes the distance to the reference path returns natural parameters with the values $\mu = 0.30$ and $k = -0.1996$, which are close to the exact values corresponding to the true periodic orbit. As the constant time interval between neighboring nodes is reduced further, the returned value of k approaches the true value of $k = -0.20$. In addition, note that the converged discrete path does not exactly reflect a periodic orbit in the continuous time system, but rather an approximation. The returned solution does, however, lie sufficiently close to the original periodic orbit, thereby demonstrating the use of discrete variational mechanics in determining the natural parameters of a dynamical system that may enable a desired type of motion to exist.

Another example of the utility of discrete variational mechanics in supplementing the exploration of autonomous dynamical systems involves the search for a periodic orbit in the CR3BP that approximately resembles a given orbit existing in the MCR3BP. Such analysis may be useful in exploring and isolating the effect of a three-body interaction, or any other autonomous force contribution. Consider the same retrograde exterior orbit existing in the MCR3BP for $\mu = 0.30$ and $k = -0.20$, with an orbital period of $T = 26.26$. This reference path is discretized into 500 nodes and depicted in Figure 6(a) using black dots. Given that k possesses a nonzero value below the critical value of $k = -0.1985$, neither of the triangular equilibrium points exist. Of course, since the selected orbit exhibits pointed loops in the vicinity of the location at which these equilibrium points would exist in the CR3BP, this particular orbit from the MCR3BP may not be exactly reproducible in the CR3BP. Rather, the goal of this example is to determine if an orbit resembling this reference path in terms of its general geometry exists in the CR3BP, as well as the required value of μ. To achieve this goal, the discrete path in Figure 6(a) is supplied as a reference path for the constrained optimization problem formulated using discrete variational mechanics. When searching for a locally minimum solution that resembles this periodic orbit, the value of k is held constant at $k = 0$, consistent with the CR3BP, while the time step (and, therefore, the orbital period), the mass ratio and the path itself are all treated as variables. Without a lengthy continuation process in both natural parameters, which may not necessarily be successful, the value of μ at which a similar family of orbits might exist in the CR3BP is unknown. Furthermore, the

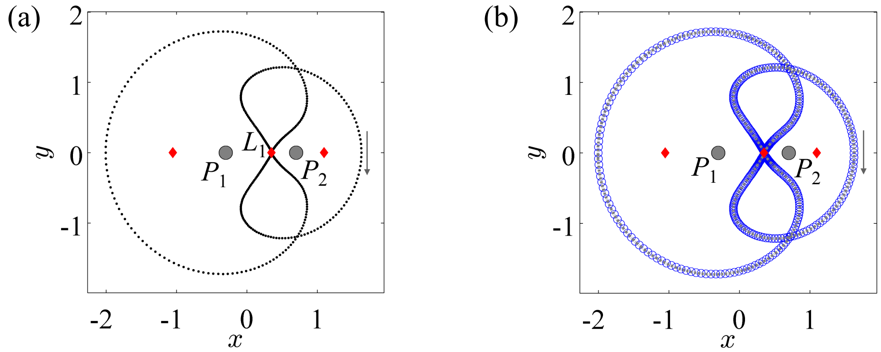

Figure 5: Recreating an orbit in the retrograde exterior family: (a) reference path with $\mu = 0.30$, $k = -0.20$, and (b) discrete path for $\mu = 0.30$, $k \approx -0.1996$.

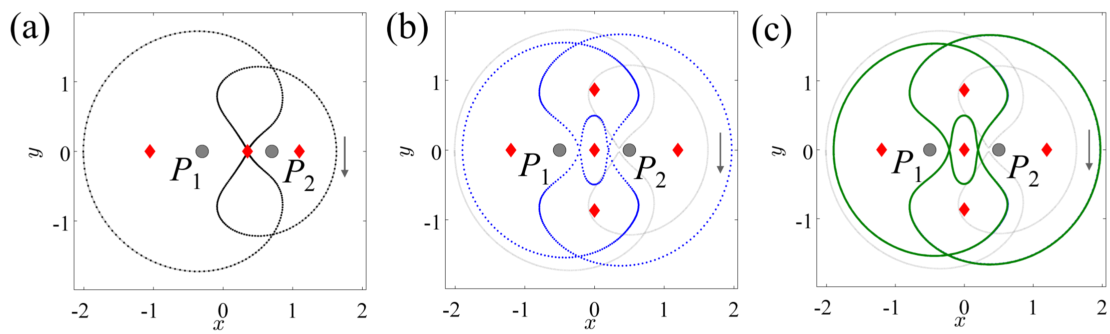

Figure 6: Recreating a retrograde exterior orbit: (a) reference path (black) for $\mu = 0.30$ and $k = -0.20$, (b) closely reproduced in the CR3BP for $\mu = 0.50$ by a discrete path (blue), and (c) verified to exist near a continuous periodic orbit (green) in the CR3BP at $\mu = 0.50$.

addition of the three-body interaction directly modifies the acceleration field, and, therefore, the velocities and periods of any orbits with a similar geometry in the CR3BP. To accommodate this effect, 500 unique initial guesses are input to the constrained optimization problem that is implemented using the sequential quadratic programming algorithm available in Matlab's *fmincon* routine. Each initial guess is constructed using the reference path with a small amount of random noise applied to the position variables at each node. In addition, each initial guess for μ is randomly selected to lie somewhere in the range $\mu = [0.10, 0.50]$, while the initial guess for the time step variable, h, lies within 25% of the value of h along the reference path. The constrained optimization problem is then solved, with $k = 0$ incorporated as an equality constraint, for each of these 500 guesses and the best locally optimal solution is selected.

The constrained optimization problem as formulated via discrete variational mechanics is leveraged to explore the selected retrograde exterior orbit that exists in the MCR3BP and deduce if it is approximately reproducible in the CR3BP. The best converged solution is plotted with blue dots and overlaid on the original reference orbit (gray) in Figure 6(b). Note that the primaries and equilibrium points indicated in this plot correspond to $\mu = 0.50$, the mass ratio at which the converged solution exists in the CR3BP. This locally optimal solution also possesses a period of $T = 25.89$, which is slightly lower than the orbital period of the reference orbit. Although the computed solution is an approximation, it is straightforward to verify that this discrete path exists close to a continuous periodic orbit at $\mu = 0.50$ in the CR3BP. A nearby continuous periodic orbit, computed using a multiple shooting algorithm, is overlaid in green in Figure 6(c) and closely matches the computed discrete path. As expected, the presence of the three-body interaction impacts both the position and velocity along an orbit. Correspondingly, the converged orbit does not exactly follow the same path as the reference orbit. Furthermore, the loops around L_4 and L_5 for this converged solution in the CR3BP encompass the location of L_1, rather than exhibiting pointed tips that are characteristic of the reference path. This inconsistent behavior of the orbit close to L_1 can likely be attributed to a difference in the stability of the collinear equilibrium point for the dynamical environments corresponding to the reference and computed solutions. In fact, the periodic orbit for $\mu = 0.50$ and $k = 0$, plotted in green in Figure 6(c), encircles L_1 in a direction and shape that resembles the L_1 Lyapunov family itself. Recall that the L_1 Lyapunov family of orbits does not exist for $\mu = 0.30$ and $k = -0.20$. Accordingly, the 'pointed tips' along the reference orbit in the MCR3BP are a reflection of the absence of any oscillatory modes about L_1. Thus, while the exact characteristics of the motion along the reference orbit are not reproducible in the CR3BP, a similar geometry is certainly achieved. This observation, resulting from the complementary use of both composite stability representations and discrete variational mechanics, suggests that while large retrograde orbits of a given geometry may be inherited from the CR3BP, the presence of a three-body interaction may significantly affect their characteristics relative to the primaries in a binary system. Such key differences may supply insight into the presence of any unique effects of the selected autonomous force contribution.

Prograde Circumstellar Orbits Encircling the Largest Primary

One type of simply-periodic circumstellar motion that encircles the larger primary, P_1, includes two families of prograde orbits. These two families, plotted in Figure 7 at a sample mass ratio equal to $\mu = 0.30$, are labelled 'family 1' and 'family 2'. The location of the largest primary is marked by a gray filled circle and the direction of motion for both families is indicated by the arrows. Although each family evolves with the mass ratio in an intriguing manner that is evident in their composite stability representations and can be clarified using the stable and unstable manifolds emanating from the L_1 Lyapunov orbits, only 'family 1' is explored in this investigation.[7]

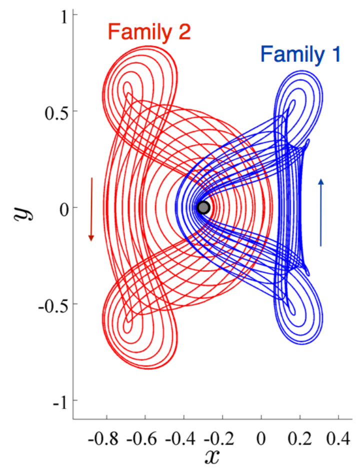

Figure 7: Sample members of prograde orbits in 'family 1' and 'family 2'.

To examine the evolution of 'family 1' in the CR3BP, the in-plane stability index is first examined over various mass ratios. As evident in the stability representation in Figure 8(a), the family becomes closed (with the upper and lower bounds on the period indicated by the gray shaded regions) and disappears as the mass ratio approaches the value of $\mu \approx 0.26284$. The in-plane stability curves for selected mass ratios close to this critical μ value are plotted as a function of the period in Figure 9, with dotted lines located at $s = +2$ and $s = -2$. In this figure, it is clear that, for each period, two orbits exist in 'family 1' for the corresponding values of μ. As the mass ratio is further decreased towards the critical value, the minimum along the stability curve rises and passes through $s = -2$, causing the two period-doubling bifurcations at $s = -2$ to eventually disappear, with a stable periodic orbit existing at each value of the period across the family. Thus, small blue structures appear at the bottom of the composite stability representation in Figure 8(a). Eventually, the two tangent bifurcations at the minimum and maximum period of the family collide, and the family no longer exists. The physical interpretation of this collision of bifurcations has been explored in previous work using the manifolds of orbits in the L_1 Lyapunov family.[7] Assuming that the dynamical environment near a binary star is adequately modeled by the CR3BP and that close approaches to the primaries are allowable, the disappearance of 'family 1' at the critical μ value suggests that an exoplanet would not exhibit the behavior typical of this particular family near a binary star with a mass ratio below $\mu \approx 0.26284$. There could, however, be some type of prograde motion that an exoplanet orbiting P_1 could exhibit for mass ratios below $\mu \approx 0.26284$, as long as the observed or hypothesized motion is not consistent with orbits belonging to 'family 1'. In addition to the termination of 'family 1', the composite stability representations reveal a discontinuity in the stability indices corresponding to 'family 1' at another critical mass ratio: $\mu \approx 0.4232$. As explored in previous work, two tangent bifurcations at $s = +2$, occurring in both 'family 1' and 'family 2' meet as μ approaches this critical

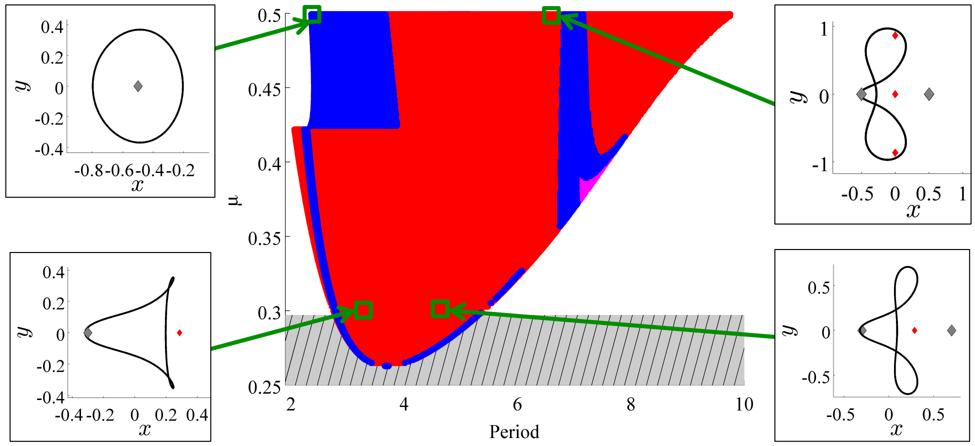

(a) In-plane stability.

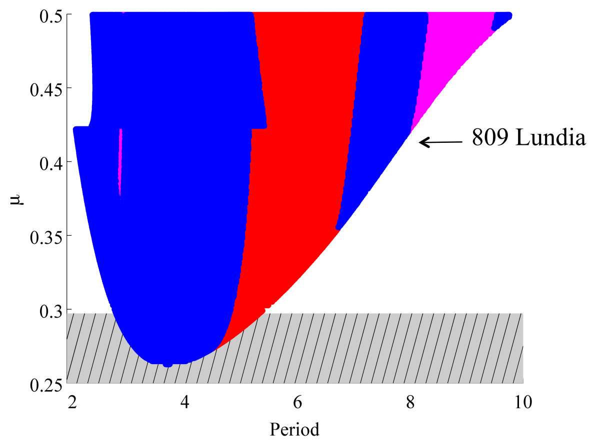

(b) Out-of-plane stability.

Figure 8: Stability representation for 'family 1' in the CR3BP, comprised of prograde orbits about P_1. Orbital stability is indicated via color: stable (blue), positive unstable (red), and negative unstable (purple).

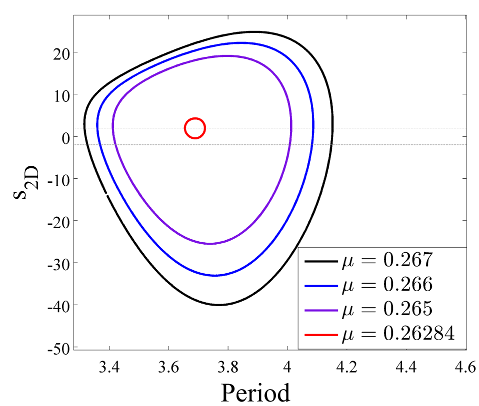

Figure 9: In-plane stability index for 'family 1' at selected values of the mass ratio near $\mu = 0.26284$.

mass ratio, yielding a collision of bifurcations.[7] For mass ratios near $\mu = 0.4232$, branches along each of the prograde families are exchanged, resulting in a structural change along the family in the CR3BP.

Since 'family 1' exists in the CR3BP for $\mu = 0.30$, the evolution of this family of orbits is also examined in the MCR3BP. The resulting composite stability representations appear in Figures 10(a) and 10(b) for the in-plane and out-of-plane stability indices, respectively. Although this investigation considers values of the constant scaling factor representing the three-body interaction within the range $k = [-0.20, 0.70]$, this family only appears to exist for $k \approx [-0.0139, 0.1866]$. To understand these bounds on the value of k, first consider the case of a repulsive three-body interaction. With increasingly negative values of k, this family becomes closed and the two tangent bifurcations occurring at the minimum and maximum orbital periods approach each other. These tangent bifurcations collide at $k \approx -0.0139$, and the family disappears. Considering both the in-plane and out-of-plane stability, comparison of Figures 8 and 10 indicates that the effect of a repulsive three-body interaction on the existence and stability of this prograde family of orbits is qualitatively similar to the effect of decreasing the mass ratio below $\mu = 0.30$. When the three-body interaction is attractive, however, two discontinuities appear in the colored structures for the planar stability in Figure 10(a). These discontinuities are not numerical artifacts; rather, they reflect the occurrence of structural changes along the family. The first discontinuity occurs at $k \approx 0.01$, with a larger blue region of stable periodic orbits appearing at lower orbital periods. As in the CR3BP, this family often possesses two members at a given value of the orbital period. At $k \approx 0.01$, a small purple region also appears from behind the red and blue structures that are brought to the front in the plot, indicating that the family might no longer be closed. To explain these discontinuities, analysis of the in-plane stability index along 'family 1' reveals that by varying k, a local minimum in the stability index approaches the critical value $s = +2$ from above. At a critical value of k, a collision of tangent bifurcations occurs between two separate families as they exchange branches, thereby resulting in a discontinuity in the composite stability representation. As k is increased further, the blue structures corresponding to stable periodic orbits become smaller. Once k reaches another critical value, $k \approx 0.058$, the family can be confirmed to be closed and a discontinuity appears in the blue structure, corresponding to periodic motion that is stable with respect to planar perturbations at higher orbital periods. In fact, the stable region encompasses a wider range of orbital periods than at lower values of k and even in the CR3BP for mass ratios close to $\mu = 0.30$. Further increasing the strength of the attractive three-body interaction, the two tangent bifurcations at the minimum and maximum orbital periods approach and eventually collide at $k \approx 0.1866$, causing the family to cease to exist. Examination of the out-of-plane stability in Figure 10(b) for positive values of k reveals a significant departure from the effect of varying the mass ratio. In comparison to the CR3BP, a larger portion of the family is stable to perturbations normal to the orbital plane for the values of $k > 0$ at which it exists. In addition, the structures corresponding to unstable orbits encompass a smaller range of periods. Together, these observations suggest that the evolution of the selected prograde family about P_1 appears quite sensitive to the presence of a three-body interaction.

Further insight can be gained from the plots of selected orbits in the margins of Figure 10(a), as viewed in the rotating frame. The physical configuration of orbits in this prograde family appear to be dependent upon the sign of k. For instance, orbits along this family tend to exhibit loops near L_4 and L_5. When the three-body interaction is attractive and the family disappears, the loops along the limiting orbit appear nearly above and below the largest primary. However, as the value of k becomes increasingly negative towards $k = -0.0139$, the limiting orbit possesses loops that are skewed towards P_2. This difference in the appearance of the limiting orbits at the minimum and maximum values of k for which this family exists can be attributed to both the change in the dynamical field due to the presence of the three-body interaction and the sequence of branch exchanges occurring during each collision of bifurcations as k increases or decreases away from zero.

Given the sensitivity of the evolution of the prograde orbits in 'family 1' to changes in μ and k, discrete variational mechanics is used to supplement the exploration of this family by recreating an orbit at a mass ratio not encompassed by this family in the CR3BP, and allowing k to be nonzero. By employing the discrete variational formulation to approximately recreate this type orbit, the use of a lengthy continuation process in both natural parameters, which may be unsuccessful or computationally expensive, is avoided. Recall that this particular family of simply-periodic prograde orbits does not exist for mass ratios below $\mu \approx 0.26284$ in the CR3BP. However, assume that an exoplanet was discovered to move along a path resembling this type of

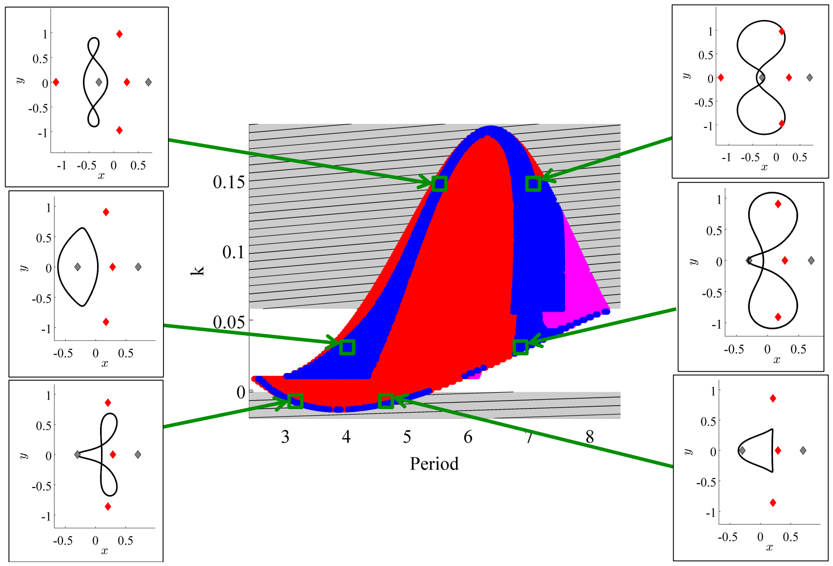

(a) In-plane stability.

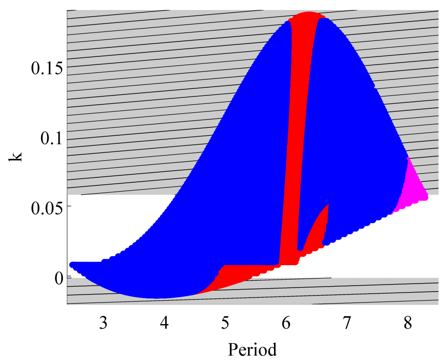

(b) Out-of-plane stability.

Figure 10: Stability of selected prograde orbits about P_1 for $\mu = 0.30$, $k = [-0.0139, 0.1866]$. Orbital stability is indicated via color: stable (blue), positive unstable (red), and negative unstable (purple).

prograde motion about the larger primary in a binary star. Also assume, for this example, that the value of the mass ratio of this binary is accurately known to equal $\mu = 0.25$. The prograde motion typical of this family may not be followed by an object in the CR3BP, since this particular family does not exist at $\mu = 0.25$. This type of periodic motion may, however exist in the MCR3BP at $\mu = 0.25$ for some nonzero value of k.

To determine the value of k at which the periodic motions typical of the prograde family of interest may exist for $\mu = 0.25$, a periodic reference path from the CR3BP is discretized and used as an initial guess in the constrained optimization problem as formulated with discrete variational mechanics. An orbit is selected from 'family 1' at a sample mass ratio in the CR3BP and discretized into 600 nodes to supply a reference path that is representative of motion along this family. The selected discrete path, plotted in Figure 11(a) using black dots, exists at a mass ratio of $\mu = 0.274625$ and possesses an orbital period of $T = 2.97$ nondimensional time units. In this figure, P_1 is located using a gray filled circle, while equilibrium points are indicated by red diamonds. As with the previous example, 500 initial guesses are constructed using the reference path with a small amount of noise. Furthermore, each initial guess is given a mass ratio of $\mu = 0.25$, while the value of k is randomly selected within the range $k = [-0.20, 0.70]$ and the initial guess for the time step variable, h, lies within 25% of the value of h along the reference path. Each initial

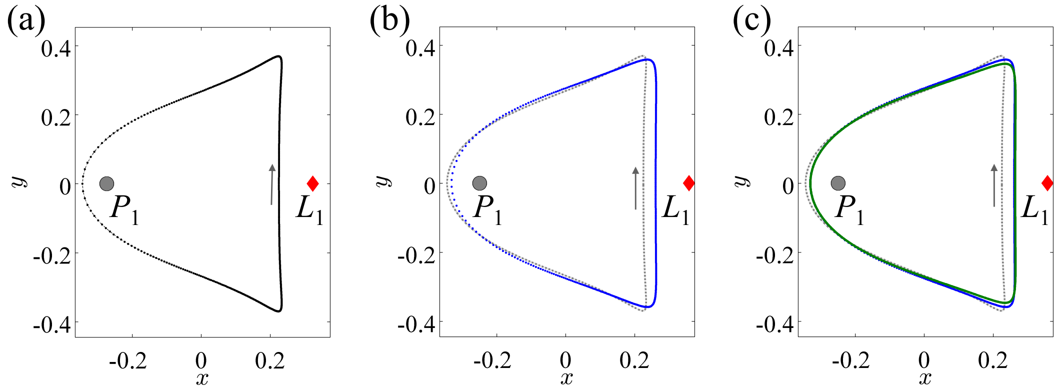

Figure 11: Prograde orbit from 'family 1' in the rotating frame: (a) discretized reference path (black) for $\mu \approx 0.274625$ in the CR3BP, (b) discrete approximation (blue) of a periodic orbit existing at $\mu = 0.25$ and $k = 0.01134$, and (c) a continuous periodic orbit (green) corrected using the discrete path (blue).

guess is used in Matlab's *fmincon* routine to construct a locally optimal solution close to the reference path. The best locally optimal solution, existing closest to the reference orbit in configuration space, is retained and plotted using blue dots in Figure 11(b). The locations of the larger primary and L_1 now reflect the new values of the natural parameters corresponding to this particular solution, which exists at $\mu = 0.25$ and $k = 0.01134$, with a period of 2.915 nondimensional time units. Note that the computed solution is simply an approximation to a continuous periodic orbit. Accordingly, a verification step is completed using a multiple shooting method to ensure that a periodic orbit exists in the vicinity of the converged discrete path in the prescribed dynamical environment. The resulting orbit, that is periodic in the continuous time system, is represented by a green solid line in Figure 11(c). Note that in this figure, the maximum y-excursions along the orbit differ slightly between the continuous and discrete paths. This discrepancy occurs due to the high orbital speed near the closest approach to P_1, which may not be accurately approximated using a first-order finite differencing. Increasing the number of nodes used to the discretize the orbit reduces this discrepancy between the continuous and discrete motion. However, nodes added to this path mostly congregate near the maximum y-excursions where the velocities are significantly slower than near periapsis. Accordingly, such orbits would benefit from time-adaptive stepping to reduce the computational expense associated with using an excessively large number of nodes. Nevertheless, the discrete variational formulation accurately predicts the presence of periodic orbits at this combination of the natural parameters, (μ, k). Furthermore, the results of this example suggest that, in the presence of a small three-body interaction, prograde periodic motion typical of 'family 1' may be observed in binary systems with mass ratios at which the family does not normally exist in the CR3BP. Such analysis thereby demonstrates the utility of discrete variational mechanics as a supplement to stability analysis when understanding the effect of an additional autonomous force contribution added to the CR3BP. In addition, such analysis may aid in identifying key signatures of additional force terms when investigating systems with an accurately known mass ratio.

SUMMARY

The influence of a three-body interaction on periodic orbits in the restricted problem is explored using a combination of both stability analysis and discrete variational mechanics. The composite stability representation employed in this investigation offers a clear and simple method for visualizing the stability of a family of orbits across various mass ratios in the CR3BP, as well as under the influence of an additional autonomous force of various strengths. These figures, which resemble the exclusion plots often employed in physics, allow for the detection of structural changes in a family and an evaluation of the orbital periods corresponding to stable or unstable members across a range of each natural parameter describing a dynamical system. Such analysis is completed in both the CR3BP and the MCR3BP for simply-periodic retrograde orbits that exist in the exterior region and simply-periodic orbits that encircle the largest primary in a prograde direction. As a supplement to the stability analysis used to study the evolution of a family, discrete variational mechanics is employed to determine whether a given reference path is reproducible in a system that is described by a different set of natural parameters. In particular, a constrained optimization problem is formulated and solved to find discrete approximations to periodic orbits along with the corresponding values of μ and k describing the dynamical environment. In combination, both stability analysis and discrete variational mechanics are used in this investigation to explore the influence of an autonomous force added to the restricted problem, and to determine whether its effects are approximately reproducible by varying the mass ratio.

ACKNOWLEDGMENT

The authors wish to acknowledge support from the Zonta International Amelia Earhart Fellowship during this work, as well as the School of Aeronautics and Astronautics at Purdue University.

REFERENCES

[1] J.L. Margot, M.C. Nolan, L.A.M. Benner, S.J. Ostro, R.F. Jurgens, J.D. Giorgini, M.A. Slade, D.B. Campbell, "Binary Asteroids in the Near-Earth Object Population," *Science*, Vol 296 no. 5572, 2002, pp. 1445-1448.

[2] D. Raghavan, T.J. Henry, B.D. Masion, J.P Subasavage, W. Jao, T.H. Beaulieu, N.C. Hambly, "Two Suns in the Sky: Stellar Multiplicity in Exoplanet Systems," *The Astrophysical Journal*, Vol. 646, 2006, pp. 523-542.

[3] L. Chappaz, "Bounded Motion Near Binary Systems Comprised of Small Irregular Bodies," *AIAA/AAS Astrodynamics Specialist Conference*, August 2014, San Diego, California.

[4] E. Fischbach, Long-Range Forces and Neutrino Mass, *Annals of Physics*, vol. 247, pp. 213-291, 1996.

[5] N. Bosanac, "Exploring the Influence of a Three-Body Interaction Added to the Gravitational Potential Function in the Circular Restricted Three-Body Problem: A Numerical Frequency Analysis", M.S. Thesis, School of Aeronautics and Astronautics, Purdue University, West Lafayette, Indiana, 2012.

[6] E. Fischbach, C.L. Talmadge, *The Search for Non-Newtonian Gravity*, New York: Springer-AIP, 1999.

[7] N. Bosanac, K.C. Howell, E. Fischbach, "Stability of Orbits Near Large Mass Ratio Binary Systems," *2nd IAA Conference on Dynamics and Control of Space Systems*, March 2014, Roma, Italy. IAA-AAS-DyCoSS2-14-05-08.

[8] D. Benest, "Effects of the Mass Ratio on the Existence of Retrograde Satellites in the Circular Restricted Problem: IV. Three-dimensional Stability of Plane Periodic Orbits," *Astronomy and Astrophysics*, Vol. 54,1977, pp. 563-568.

[9] A. Moore, "Discrete Mechanics and Optimal Control for Space Trajectory Design," Ph.D Thesis, Control and Dynamical Systems, California Institute of Technology, Pasadena, California, 2011.

[10] N. Bosanac, K.C. Howell, E. Fischbach, "Exploring the Impact of a Three-Body Interaction Added to the Gravitational Potential Function in the Restricted Three-Body Problem," *23rd AAS/AIAA Space Flight Mechanics Meeting*, February 2013, Hawaii. AAS 13-490.

[11] V. Szebehely, *Theory of Orbits: The Restricted Problem of Three Bodies*. London, UK: Academic Press, 1967.

[12] C.N. Douskos, "Effect of Three-Body Interaction on the Number and Location of Equilibrium Points of the Restricted Three-Body Problem," *Astrophysics and Space Science*, December 2014.

[13] T.S. Parker, L.O Chua, *Practical Numerical Algorithms for Chaotic Systems*. New York: Springer-Verlag, 1989.

[14] G. Contopoulos, *Order and Chaos in Dynamical Astronomy*. Germany: Springer-Verlag, 2002.

[15] W. S. Koon, M. W. Lo, J. E. Marsden, S. D. Ross, *Dynamical Systems, the Three Body Problem and Space Mission Design*, 2006.

[16] L. Perko, *Differential Equations and Dynamical Systems*. Third Edition, New York: Springer, 2000.

[17] R. Seydel, *Practical Bifurcation and Stability Analysis: From Equilibrium to Chaos*. New York: Springer-Verlag, 1994.

[18] S. Ober-Blobaum, O. Junge, J.E. Marsden, "Discrete Mechanics and Optimal Control: An Analysis," *ESAIM: Control, Optimization and Calculus of Variations*, Vol. 17, Issue 02, April 2011, pp. 322-352.

[19] D.T. Greenwood, *Principles of Dynamics, Second Edition*. New Jersey: Prentice-Hall,1988

[20] C. Lanczos, *The Variational Principles of Mechanics*. Toronto: Courier Dover Publications, 2012

[21] J.E. Marsden, M. West, "Discrete Mechanics and Variational Integrators," *Acta Numerica* Vol 10, pp. 357-514, 2001.